APD imaging probe for tritium surface contamination

Richard A. Myers*[a], Richard Farrell[a], Frank Robertson[a], David Dogruel[b] and R. Scott Willms[b]
[a]Radiation Monitoring Devices, Inc., 44 Hunt Street, Watertown, MA, USA 02472
[b]Los Alamos National Laboratory. Mail Stop J964, Los Alamos, NM, USA 87544

ABSTRACT

We report on the development of a practical, easy-to-use, multi-element, solid-state instrument for detecting and imaging tritium contamination on surfaces. The innovation, which enables this instrumentation, relies on cutting-edge silicon avalanche photodiode (APD) array detector technology to provide an effective coverage area without compromising the overall sensitivity. We discuss the design and assembly of a prototype unit to monitor a surface area of over 900 mm^2 while maintaining a spatial resolution of less than 4 mm. During tests at Los Alamos National Laboratories, we demonstrated tritium counting efficiencies of over 40% and established that this unit can be used to expedite established testing procedures by locating areas of potential activity or when combined with established swipe analysis.

Keywords: Tritium, Avalanche photodiode, beta detection

1. INTRODUCTION

1.1 Motivation

The monitoring systems at all nuclear power plants, US Department of Energy (DOE) facilities and other international agencies handling radioactive materials are critically important to their safe operation. Personnel at these facilities need to be informed of the environmental status and provided warning of dangerous conditions so that protective measures and rapid corrective action may be taken. Surveillance of the location and the degree of air and surface contamination are important to prevent accidental uptake of hazardous materials by personnel. Measurements at radiological boundaries are particularly important to determine whether or not items can be released for use outside of the facility.

Although the majority of radiological materials can be easily characterized, the low radiation energy of tritium (^3H) presents unique challenges for its health-risk assessment. In the environment, tritium readily replaces hydrogen molecules, thereby distributing it widely on a global scale. Furthermore, tritium absorbed into humans through respiration, ingestion and diffusion through the skin may cause cancer, genetic mutations, and developmental defects in unborn children. While tritium incorporated into water only has about a 10-day half-life within the body, if workers inhale tritiated particles into the lungs, the tritium can remain within the body much longer and result in dramatically higher radiation doses. In addition, no threshold or "safe dose" of tritium has been scientifically established for any of these effects [1].

The difficult in detecting tritium is especially acute in facilities that are being shutdown. Because tritium can be readily absorbed onto most metal surfaces, including those made from steel, aluminum and plastics it is released into the atmosphere when heated at high temperatures. During decommissioning operations, there is greater risk that stable metal tritide particulate will be liberated as normally sealed equipment and gloveboxes are being opened, handled, characterized and packaged for disposal. While airborne tritium particles can be delivered to the detector where analysis is relatively well established, there are presently no good methods for surface analysis before these releases occur.

1.2 Tritium and Tritium Detection

Radioactivity in tritium involves the emission of an energetic electron, or a beta particle, and a coincident emission of a neutrino. With a lifetime of 12.3 years, tritium is the weakest beta emitter known. The average energy of a beta electron resulting from this decay is ~ 5.6 keV, making its detection extremely difficult. These low energy betas penetrate only fractions of a micron into most solid materials and have a range of less than 3 mm in air. For health or safety

Penetrating Radiation Systems and Applications IX
edited by F. Patrick Doty, H. Bradford Barber, Hans Roehrig, Richard C. Schirato
Proc. of SPIE Vol. 7080, 70800C, (2008) · 0277-786X/08/$18 · doi: 10.1117/12.800763

implications, an indication of loose, removable tritium contamination is of considerable concern. Because of the uncertain health effects resulting from exposure to tritium, the existing free-release limits at DOE facilities range from 1,000 to 10,000 dpm/100 cm^2.

Loose contamination is routinely monitored by smears, which are wiped over a surface by a trained technician and then analyzed by liquid scintillation or proportional counting. While very sensitive, this method is operator dependent, creates radioactive waste and results in the destruction of the samples. The most obvious drawback is the inherent variability in collecting the swipe sample. Another drawback is the time required evaluating the swipes and then returning the results to facility personnel. In some cases (such as the free release of equipment from controlled facility), no further work can be performed until these results are returned. Often, when there is a backlog of samples or lack of trained technicians, the testing can take several days.

One method envisioned for monitoring tritide particles involves their collection on the filter surfaces followed by evaluation using a real-time monitor to measure the amount of tritium accumulated. Such a monitor must be portable and very sensitive since even small amounts of tritium may be dangerous. While particulate collection equipment has already been developed, monitors that meet the required criteria are very limited. A second method of detection would be to directly count the beta decays using a solid-state detector that is positioned in close proximity to the sample. Unlike methods that rely on sample removal, direct detection offers the capability to monitor fixed contamination as well as the loose particulates.

A particularly promising instrument for direct-detection of beta emission is a sensor using a large area solid-state detector. Such a system can provide far higher sample throughput for a wide variety of tritiated samples as well as for other beta emitting radiolabels, by eliminating much of the sample preparation and by increasing the speed of the measurement. Solid-state detectors would also provide imaging capabilities, further improving the analysis of contaminated surfaces. Programs that require the mapping of tritium include fusion sciences where localized deposits on tiles can help determine problems with plasma confinement. In addition, imaging the distribution of tritium on a surface can give further information as to the source of the contamination.

Presently, one of the most versatile single-element detectors is the silicon PIN photodiode [2]. Researchers have used these photodiodes, such as those manufactured by Amptek, Inc. (Bedford, MA) to monitor tritium levels directly on flat surfaces in real time [3]. Silicon is highly responsive to beta energies below ~ 25 keV and does not require protective windows that would absorb the low energies. The primary disadvantage of the device is the small size (< 15 mm^2) of the detector and its relatively poor sensitivity compared with liquid scintillation counters. As the area of a photodiode increases, so does the detector's capacitance and, eventually, the higher noise current limits the usefulness of the larger area. However, the advantage of real time energy resolution for discrimination of radioactive species makes the photodiode an attractive alternative to the liquid scintillation counters.

An alternative to the PIN photodiode is the silicon avalanche photodiode (APD) [4]. These solid state detectors function in the same manner as PIN photodiodes but with the benefit of internal gain, which provide improved sensitivity. APDs were first considered for monitoring beta radiation over thirty-five years ago and several research efforts have explored their use as detectors for tritium [5-8]. Unlike the PIN photodiodes, the most recent generation of APD detectors are responsive to tritium contamination below the DOE free release limits [9].

1.3 Avalanche photodiodes

An APD is essentially a diode operated at very high reverse bias. The physical mechanism forming the avalanche gain occurs when a photoinduced-electron acquires enough energy from a sufficiently strong applied electric field to excite new carriers by the process of impact ionization. The additional carriers in-turn, can obtain sufficient energy from the electric field to cause further impact ionization, creating an avalanche of carriers [10]. The increased current resulting from the avalanche process is the primary advantage of an APD over a conventional, unity gain photodiode.

Silicon APDs made through a deep diffusion process can operate with gains of over 1,000 at room temperature and 10,000 when cooled [11]. By carefully controlling the doping parameters that are used to form the p-n junction, extremely low values of the ionization constant (k), which is directly related to the overall APD performance, can be

achieved [12]. Because they are silicon-based devices, they have the additional advantageous feature of broad spectral sensitivity and high quantum efficiency from ~ 300 nm to 1000 nm. In addition, APDs with areas of 78 mm^2 and thickness of 0.5 mm can detect radioactive particles with energies from 3 keV to 22 keV at room temperature [9]. This is compared with energy thresholds of > 4 keV for 13 mm^2 PIN photodiodes.

Although RMD has the capability to manufacture APDs as large as 45 cm^2, the dark noise increases with the detector area and cooling is required to achieve the necessary sensitivity to tritium. On the other hand, RMD routinely fabricates pixelated arrays of APDs and the array format offers great promise for the detection of tritium on surfaces. In addition to its imaging capability, the pixels have individual readout, allowing the user to maintain the high sensitivity of a small area device while expanding the interrogation area by increasing the number of pixels. For this reason, we explored the creation of an APD-based instrument that could be used to monitor tritium on surfaces with a high degree of sensitivity and maximum coverage.

2. METHODOLOGY

2.1 APD Processing

APD arrays were made using RMD's proprietary fabrication processing procedures and depicted in Figure 1. The most important aspect in the process consisted of making patterned grooves in the n-type silicon substrate with a diamond dicing saw. That step was followed by the deep diffusion of the p-type dopant. During diffusion, the presence of the grooves produces a contoured doping profile rather than a simple layered structure. The dead layer at the surface of the device has a major effect on the tritium counting efficiency because tritium does not penetrate far into the device. Studies have shown us that our doping profile in conjunction with a reduction in the dead layer is important for achieving high tritium counting efficiencies. In addition, a final passivation layer needed to maintain a hermetic seal was determined to have a limited effect on the tritium counting efficiency.

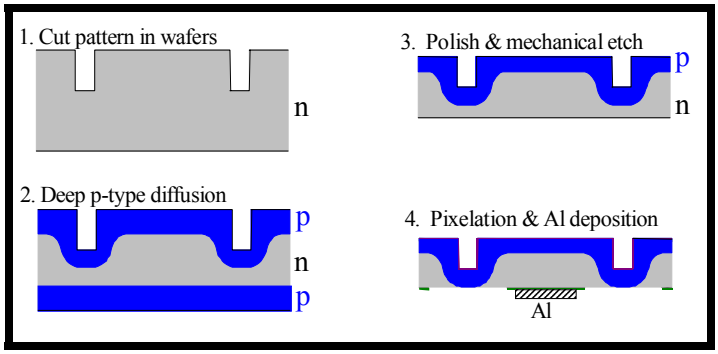

Fig. 1. Schematic drawing of steps involved in producing a planar APD array.

Following fabrication, the detectors were packaged on an alumina substrate. An underfill epoxy was used to attach the device and provide a protective seal for the back surface of the array. This process enabled us to apply a vertically orientated electrical connection, as opposed to the horizontal connection associated with wire bonding. Finally, electrical contacts were attached to the detector.

Square-shaped APD arrays were fabricated with 16-elements (4 x 4 format) at a pitch of ~ 2.48 mm, 64-elements (8 x 8 format) with a pitch of 4.32 mm and single element devices with dimensions of ~ 9 mm on a side. The groove spacing along the wafer determined the pixel pitch and the photosensitive region is reduced by ~ 0.2 mm due to the dead space between pixels. In addition, because of the slope in the diffusion profile, the active region near the pixel boundary does not reach the same maximum signal gain as that observed in the central region of the pixel. For the devices with a pitch > 4 mm, this region is only a small percentage of the total area.

2.2 Experimental procedure

APDs were characterized for dark current and responsivity. For post-amplification, we used CR-101 charge-sensitive preamplifiers designed by Cremat, Inc. (Watertown, MA) and a model 2020 spectroscopy amplifier from Canberra Industries (Meriden, CT). While these electronics are not designed for portable, multi-channel readout, they provided adjustable amplification during our analysis and promoted rapid comparison testing of several APD detectors. The amplified output was connected to a multi-channel analyzer (MCA) for display and analysis.

A measurement of each detector's active area was necessary to calibrate its counting efficiency. To do this, we scanned a focused laser light source across the surface of the device and measured the response as a function of position. We defined the active area as the full-width at half maximum (FWHM) of the response curve generated during the scan. Each pixel in the 64-element array had an active area of ~ 16 mm^2 at unity gain and 13 mm^2 at a gain of 1000. The 16-element APD array pixels were measured to have an active area of ~ 3.24 mm^2, while the single element detector had an active area of ~ 77 mm^2 at high gains.

Gain as a function of bias was measured using either optical illumination or a radioisotope with fixed X-ray energy. Care was taken to make certain that the resulting current did not saturate the amplifier output. Figures 2 shows the gain as a function of the applied bias from a representative APD pixel that was part of the 16-element APD array. The figure also contains a plot of the leakage current as a function of the applied bias when four of the APD array pixels were connected in parallel. Each pixel had an active area of ~ 4 mm^2. The total leakage current reaches 1 μA at the highest gains but was only a few hundred nA at the optimal gain setting. Although the leakage current varies with detector size, the gain curve was similar for all the APD pixels tested.

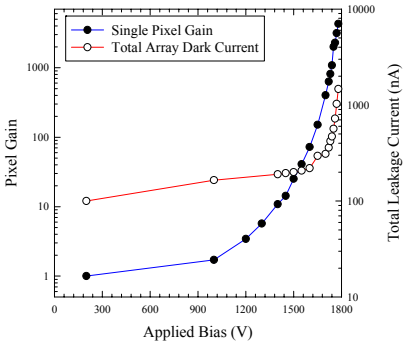

Fig. 2. Plot showing the gain and leakage current versus bias for a pixel from a 16-element APD array. The leakage current is the sum of 4 pixels connected in parallel.

2.3 Tritium detection characterization

To measure the counting efficiency of the APDs, a calibrated tritium source was purchased from AEA Technology QSA, Inc. (Burlington, MA). This source was a 100 cm^2 aluminum plate with a nominal activity of 100 disintegrations per minute (dpm) or 45 nCi. Because the tritium was embedded in the aluminum surface, direct contact between the APD and the plate did not change the activity or contaminate the detector. In addition, for higher activity, we used a tritium source embedded in a 25-mm diameter disk of polymethyl methacrylate (PMMA). The activity of the source was ~2 x 10^5 dpm from a 1 cm^2 area of the surface. Tests were also performed at Los Alamos National Laboratories with three calibrated tritium sources with nominal activities of 100,000 dpm/100 cm^2, 10,000 dpm/100 cm^2 and 1000 dpm/100 cm^2.

The APD detectors tested had similar tritium counting. A careful investigation demonstrated that a single-channel APD unit with a 77 mm^2 APD had an efficiency up to 45% when there was near-zero separation between the detector and the tritium source. When the APD was mounted with a source-detector separation distance of ~ 0.5 mm a counting efficiency of ~ 30% was measured.

2.4 Comparison with PIN photodiode

We compared the performance of our APD to that of a windowless PIN photodiode from Amptek by measuring their responses to a ^{55}Fe X-ray source and a tritium source. Figure 3 shows that by using the 5.9 keV peak of the ^{55}Fe, we were able to determine the energy threshold of both detectors. Although the data for each detector was collected with different MCAs, we were able to calibrate the two plots to the peak energy from the ^{55}Fe x-ray source. Both detectors had similar active areas of ~ 13 mm^2 and the APD was biased to ~ 1650 V for a gain of ~ 300. The threshold for the photodiode is ~ 4 keV, while that of the APD approaches 1 keV. The width of the ^{55}Fe energy peak is due to the

combination of several noise sources and effects of x-ray absorption. Because of the re-scaling the widths of the ^{55}Fe peak are similar for the APD and photodiode but it is not an accurate comparison of the noise of the instruments. Figure 4 shows the comparison of two tritium signals using the energy calibration of the ^{55}Fe data. A fit of the theoretical tritium energy spectrum is also given.

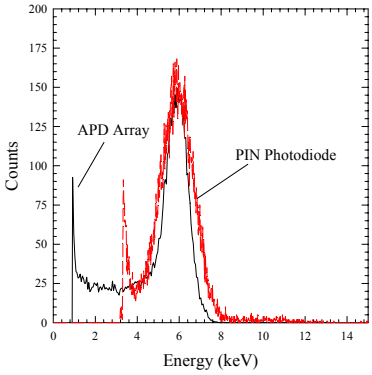

Fig. 3. Comparison of the ^{55}Fe spectrum from the RMD APD array unit and the Amptek PIN photodiode unit. The noise threshold for the photodiode is ~ 4 keV, while that for the APD is ~ 1 keV. The detectors had similar areas.

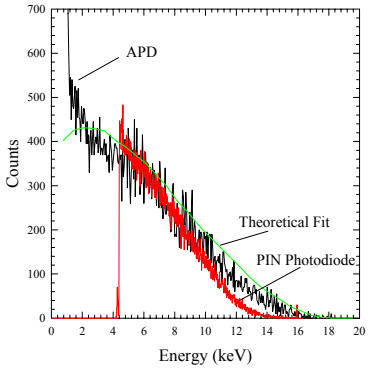

Fig. 4. Energy spectrum for tritium recorded with the PIN photodiode and the RMD APD. The thin curve is a theoretical fit.

Table 1 summarizes the results of our comparative studies between the APD and PIN photodiode. The maximum sensitivity calculations suggest the APD would be able to perform a free release measurement in ~ 1 min. A lower energy threshold is especially important for detecting beta radiation because the low energy particles comprise a significant portion of the energy spectrum. While the maximum energy of the tritium radiation is 18.6 keV, the mean is only 5.7 keV. With a threshold of 4.6 keV, the PIN photodiode can detect ~ 40% of the total spectrum, while a threshold of 1 keV to 2 keV for the APD array encompasses 88% to 77% of the events. The APD was able to detect activity from all of the calibrated sources while the PIN diode was unable to detect the activity of the plate with 1000 dpm without using very long collection times (several hours).

Table 1. Comparison of two single element APDs and PIN photodiode

Device	Active area (mm^2)	Noise Threshold (keV)	Background (Counts per minute)	Counting Efficiency	Maximum sensitivity* ($dp\sqrt{m}/100\ cm^2$)
PIN	13	4.5	12.6	15%	16,000
APD pixel	13	1.0	0.6	45%	1300
Single element	77	3.0	3.2	45%	515

* Assumes that the dark current is given by a Poisson distribution.

3. TRITIUM SURFACE DETECTION MODULE

Based on the promising experimental results for the APD array, we assembled and tested a first-generation prototype instrument designed for monitoring tritium contamination on surfaces. In addition to working as a dosimeter, the array offered imaging capabilities to determine the distribution of tritium on a surface in real-time. The module included amplification electronics, computer interface, voltage and current monitors as well software control and analysis.

3.1 APD Array

To have a coverage area of significant size, the tritium surface monitor was designed around the 64-element APD array with a pixel pitch of 4.32 mm. The resulting device would then be able to directly image a surface area of 10 cm^2, which

meant that it could be used to image the activity off an entire 1-inch swipe used at numerous DOE facilities. The potential development of a real-time swipe reader is an attractive alternative to direct surface measurement, especially when trying to examine contoured shapes.

Two monolithic arrays were packaged and tests of the individual pixels determined that the gain and dark current matched that of APDs of similar size. The arrays had < 3% pixel-to-pixel variation, a breakdown bias of ~ 1700 V and a current draw of ~ 30 μA when all the pixels were connected in parallel. Of the 120 pixels, two (both on the perimeter) had leakage currents that prevented their use. The exclusion of these two elements did not affect the characteristics of the other pixels. Figure 5 shows a picture of the fabricated and packaged 8 x 8 APD array.

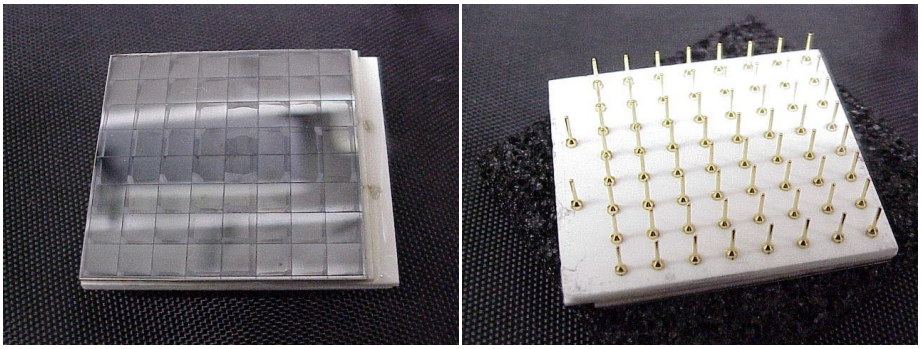

Fig. 5. Picture of the front and back sides of the 8 x 8 monolithic APD array. Each square pixel has a pitch of 4.32 mm. A ceramic backing was added to the device to allow straight-pin connections to a circuit board. Two contacts were included for the APD bias.

The tritium count rate was uniform across all of the pixels and, consequently, combining pixels into a single output channel increased the count rate proportionally. In addition, because the monitoring of 64 individual channels was excessive, we organized the pixels into groups. This allowed us to achieve a large coverage area APDs and limit the total number of output channels for easier integration with established readout electronics and low-cost A/D cards. On the other hand, combining pixels into a single channel also increased the dark current and a higher energy threshold was required to distinguish tritium counts from the background. Figure 6 shows the resulting tritium energy spectrum with 1, 2, and 4 APD pixels connected in parallel. As the number of pixels in one channel increased, the advantage gained by increasing the detector area was eventually lost because the number of beta particles with energies that fall below noise threshold decreases nonlinearly.

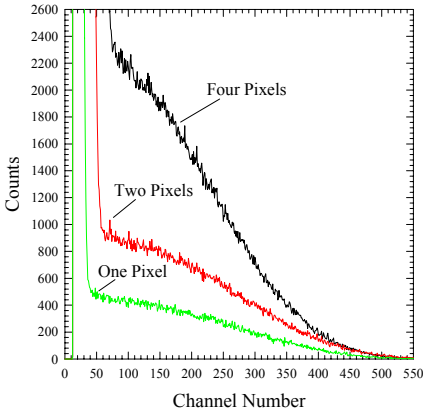

Fig. 6. Tritium energy spectra recorded using an APD array with 4.32 mm pitch. The lower trace was recorded with 1 pixel, the middle trace with 2 and the top trace with 4 pixels connected in parallel.

Based on the noise threshold as a function of the different numbers of pixels connected in parallel, the percentage of tritium particles that could be detected above each threshold, the desired spatial resolution and the available multi-channel amplification electronics, we divided the 64-element APD array into 16 output channels. The two layouts that we utilized are shown in Figure 7. One layout maintained an equivalent number of pixels (four) in each channel, while the second used a greater number of pixels on the perimeter so that the central region achieved a higher spatial resolution. The later is useful for reading of swipes, where the majority of tritium is expected to be concentrated in a ~ 1 cm^2 area near the center of the sample.

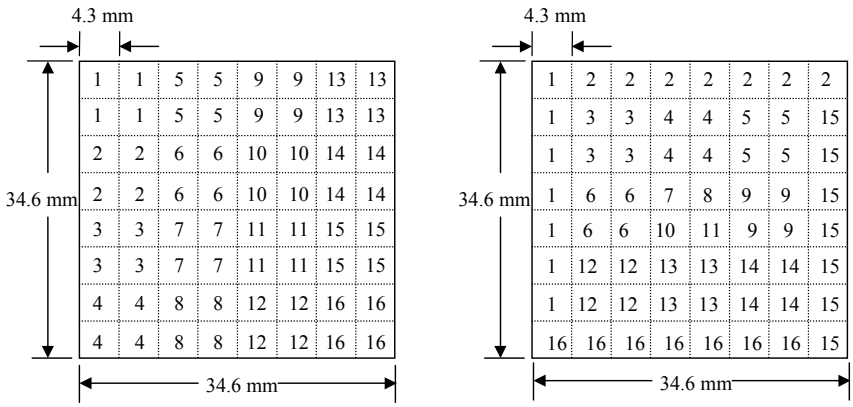

Fig. 7. Two layouts for the 8 x 8 APD array: (left) 16 channels with 4 pixels each for equivalent performance/channels and (right) 16 channels with 1 to 7 pixels per channel resulting in the highest resolution in the central region of the array.

3.2 Electronic Readout

Using ^{55}Fe source to provide a fixed source of energy at 5.9 keV, the output from each channel was monitored with an oscilloscope or MCA. Unlike most APD applications, where the high bias is applied to the common anode contact, the high voltage was then applied to the individual contacts on the backside of the array and the common front-side was connected to the electrical ground. Although this made the design more complex, it reduced the chances of shorting the high voltage to ground when the probe was in physical contact with conductive test objects. In addition, depending on the APD configuration and the number of pixels in each channel, the resistivity of each channel varied. This resulted in different gains for each channel when a common bias was applied. To match the signal outputs, limiting resistors were required at each high voltage contact. This effectively balanced the resisitivity to each channel and equalized the APD gains.

To support the simultaneous readout of the 16-channel APD array, an application specific integrated circuit (ASIC) that was developed for APD use was utilized [13]. Each ASIC chip contained 16 channels of preamplifiers, shaping amplifiers as well as the peak tracking circuitry necessary to interface with a computer. The chip was packaged onto a pin-grid array and plugged into an interface board. Careful layout and assembly of the ASIC control board was required to achieve low-noise operation. Because tritium has a continuous energy spectrum ranging from 0 to 18 keV, the ASIC output had to approach two orders of magnitude in dynamic range, so that it could preserve the energy spectrum. The ASIC has several settings, including channel gain and channel disable that were programmed through a custom software. Because the chip had to be programmed every time power was applied, a Keithley Instruments, Inc. (Cleveland, OH) PCMCIA, 12-bit A/D card was used to interface between a laptop computer and the ASIC. The Keithley card had 16-channels of analog input, four digital output channels and a single A/D converter with a bandwidth rate of 100 kHz.

To obtain enough current to power the APD and the electronics, while still maintaining a relatively portable instrument, the electronics were connected to the USB ports from the laptop computer. The 5 V power from the USB was increased to 12 V via a DC/DC converter and used to power several IC chips in the electronic readout circuit. The 12 V was also filtered and used to power a high voltage DC/DC converter from EMCO High Voltage Corporation (Sutter Creek, CA), which supplied adjustable voltages up to 2000 V at 0.5 mA to the APD. While there were larger high voltage DC/DC converters available with superior stability, the compact Unit from EMCO had low ripple and enough current for our 64-element array.

We fabricated a 4-layer ASIC board to help isolate the digital input and analog output signals. Connection was made between the power supply, ASIC and APD printed circuit boards using plug-in sockets. Figure 8 shows pictures of the three boards and an image with all of them connected in their operating configuration. The APD board has an insulating coating applied to the surface to help prevent high voltage breakdown across its surface.

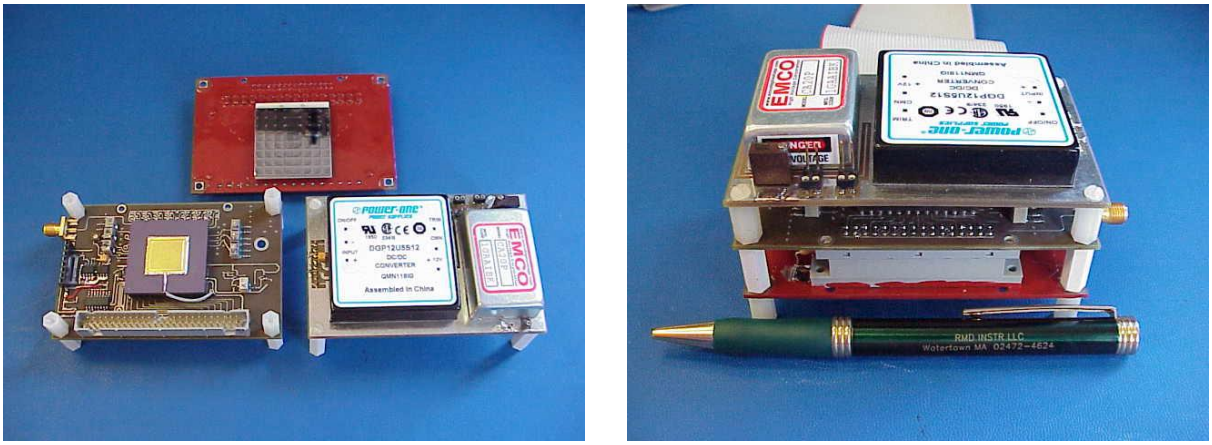

Fig. 8. Pictures of the three printed circuit boards used in the final prototype unit. The image on the left shows all three boards including the APD, ASIC and power supply. The image on the right shows all three boards coupled together for assembly in a metal enclosure. The APD board is on the bottom with the APD facing downward.

3.3 Tritium module software

To take advantage of the imaging and energy discrimination capabilities of the instrument, custom software was written to record the energy spectrum from each APD channel. The display included a color map depicting the level of activity detected by each channel, rate and time information, and the energy spectrum from the 16 channels. The 16 spectrum could be displayed simultaneously or one at a time. The program ran independently of the ASIC programming software and was compatible with either of the two APD layout geometries shown in Figure 7. The final user interface was effectively a 16-channel MCA with lower and upper energy window controls that could be set to remove noise or other unwanted events from the display. Along with the usual file options, the total counts, running time and event rate were incorporated into the user interface.

Figure 9 shows an image of the user interface when all 16-channels were viewed simultaneously and the APD array matching the layout show on the right in Figure 7. Using the color image map, it was possible to readily determine the location of "hot-spots" or if the radiation was distributed evenly. When a specific region of the array was of interest, the ASIC programming software could be used to disable select channels, reducing the total number of thermal or electronic background counts and increasing the instrument's sensitivity.

The maximum counting rate was limited by the Keithely PCMCIA readout card, which had a sampling rate of 100 kHz per channel. In order to read out all 16 channels following an event, ~ 200 μs was required before detecting the next event. This dead time resulted in a maximum count rate of 5 kHz, which is well above the highest free-release limit of tritium.

3.4 Tritium module performance

Once assembled, the APD array was recessed ~ 0.5 mm from the bottom of the probe enclosure to avoid direct contact with the surface and limit the possibility of contamination. The counting efficiency of the tritium probe in its final packaging was measured to be 10% although several pixels, when operated independently, had up to 20% counting efficiencies. This value was lower than on our preliminary studies and suggested that additional electronic noise resulting from poor shielding of the signal interface between the APD and the ASIC was a limiting performance factor.

The prototype had a background activity equivalent to 350 dpm/100 cm^2 when the tritium probe was in contact with an ordinary aluminum plate. This implied that the probe would be able to reliably monitor tritium activity as low as

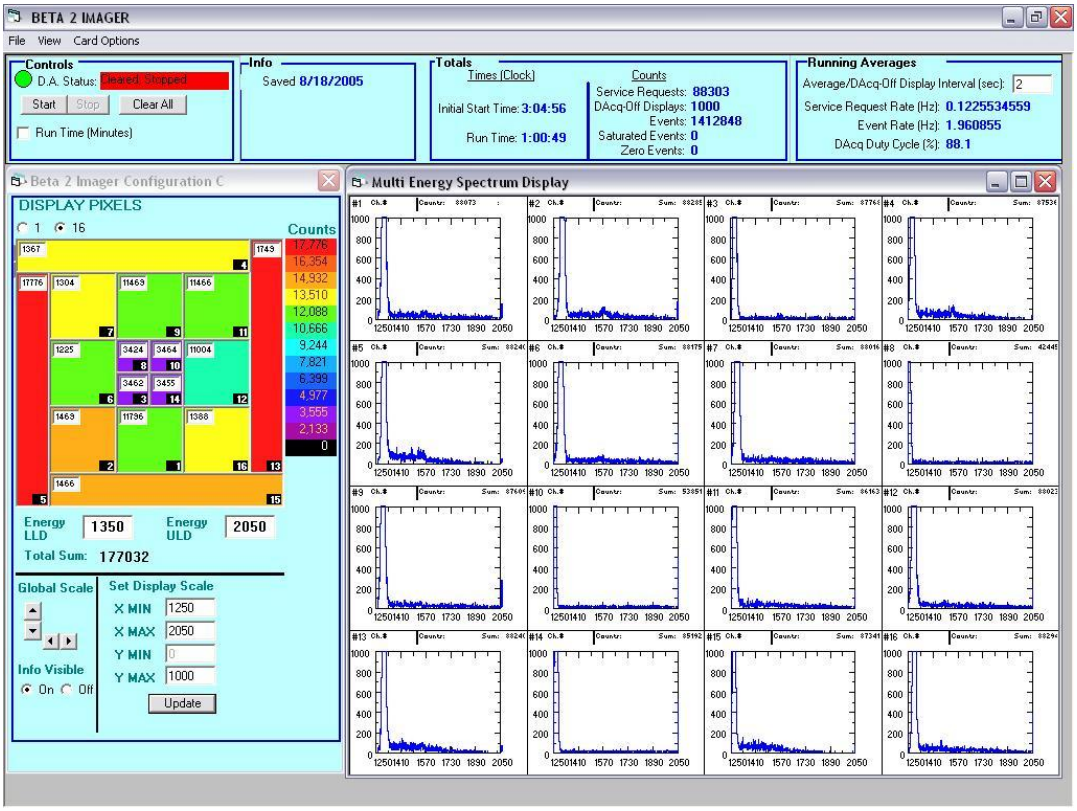

Fig. 9. Screen image following recording of tritium events collected by a 64-element APD array. On the right the energy spectrum of each channel is displayed. The color map on the left indicates the channel layout with single pixels in the center and channels with a maximum of seven pixels connected in parallel at the edges.

600 dpm (270 pCi)/100 cm^2, with appropriate settings for the APD bias and ASIC threshold. Tests at LANL confirmed that the instrument was able to positively detect a 720 dpm/100 cm^2 tritium source in less than one minute. When used as a dosimeter for detection of swipes, the count rate was consistent with those measured in an advanced liquid scintillator counter.

A picture of the final unit is shown in Figure 10. Since the APD readily responds to light, it was necessary to reduce light leakage as much as possible. The probe had two pressure switches on either side of the APD array. These switches had to be pressed in order for the bias to be applied to the APD. This helped ensure that the APD was set on a flat surface before detection was performed. Although there was also an override, if the APD was measuring an uneven surface, the unknown sample-APD distance would invalidate the calibration. Table 2 gives the performance characteristic of the tritium surface probe.

4. CONCLUSIONS

The assembly of a tritium surface probe is a significant achievement toward greater worker health assessment at DOE and other facilities that are using or once used tritium. While further work is required to establish a calibration procedure and optimize the user interface, the prototype has demonstrated the usefulness of using an APD array for real-time monitoring of tritium. In particular, it has the capabilities of meeting DOE-instituted free-release limits below 1000 dpm/100 cm^2.

Although designed for tritium analysis, the silicon-based unit is easy to operate providing real-time feedback of activity and energy from any radioactive sources with energies up to 22 keV. It can be used for pre-screening to expedite the

testing process by targeting areas of potential activity or it can be used for direct detection of tritium on surfaces, including swipe analysis. While the entire instrument is powered through the USB ports of the laptop computer, future version can utilize an application-specific user interface and a microcomputer for easier portability.

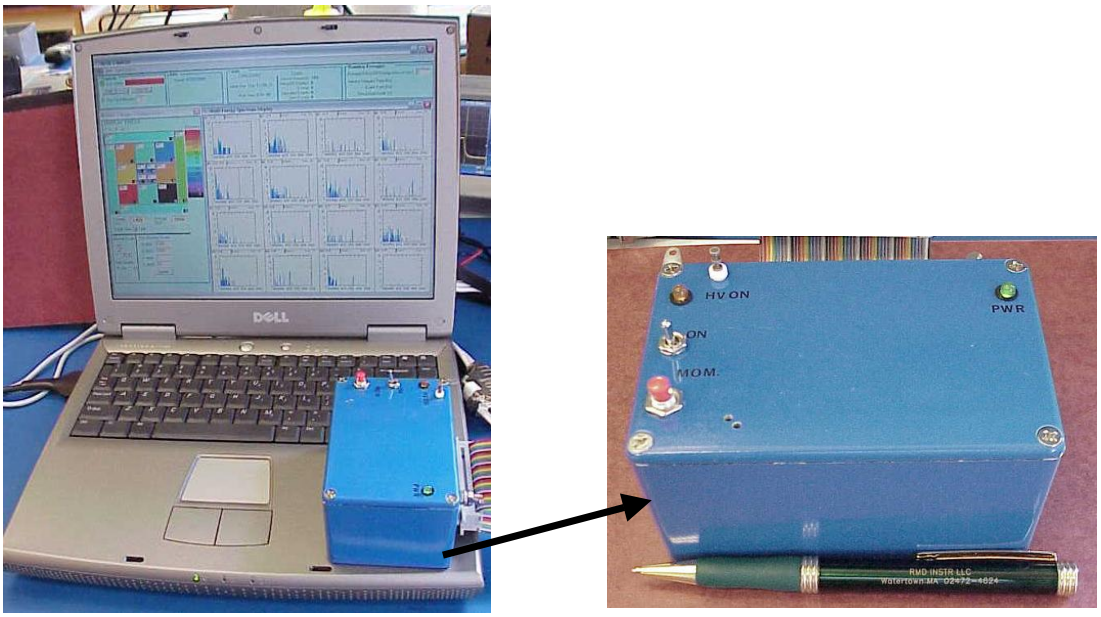

Fig. 10. Image of the tritium probe unit. The probe head contains the APD, power and ASIC boards. The APD array faces the bottom of the probe, while the top has a high voltage switch and power indicator. The size of the probe head is ~ 8 cm x 12 cm x 6 cm. The laptop is used to supply power and perform the data analysis.

Table 2. Tritium surface probe performance characteristics.

Characteristic	**Value**
Operating Temperature	22 °C
Number of Pixels	64
Number of Output Channels	16
Pixel Active Area (at 1650 V bias)	14.4 mm^2
APD Distance from Flat Surface	0.5 mm
Standard Bias Setting	1660 V
Energy Threshold	4 keV
Maximum Activity Rate	7 x 10^4 dps/100 cm^2
Maximum Spatial Resolution	3.8 mm
Background Level (entire array)	0.05 dps/pixel
Tritium Counting Efficiency	> 10%
Estimated Minimum Detectable Activity (1 minute)	600 dpm/100 cm^2

ACKNOWLEDGEMENTS

The author's gratefully acknowledge funding for the work from the United States Department of Energy through contract #DE-FG02-01ER83273. In addition, we would like to thank Mr. Greg Derderian and Dr. Gerald Entine for their considerable contributions to this work.

REFERENCES

[1] Morstin, K., Kopec, M, Olko, P., Schmitz, T. and Feinendegen, L. E., " Microdosimetry of Tritium," Health Phys. **65**, 648-656 (1993).

[2] Wampler, W. R. and Doyle, B. L., "Low-energy beta spectroscopy using pin diodes to monitor tritium surface contamination," Nuc. Instrum. Methods A349, 473 (1994).

[3] Middelhoek, S. and Audet, S. A., [Silicon Sensors], Academic Press, London, Chapter 2, (1989).

[4] McIntyre, R. J., "The distribution of gains in uniformly multiplying avalanche photodiodes: theory," IEEE Trans. Electron Devices ED-19, 703-713 (1972).

[5] Johnston, P. A., Huth, G. C. and Locker, R. J., "A solid state X-ray fluorescence analyzer for use in hostile environments," Isot. and Rad. Technol. 7, 266 (1970).

[6] McGann, W. J., Entine, G., Farrell, R. F., Clapp, A. and Squillante, M. R., "Solid-state nuclear detector for monitoring low levels of tritium," Fusion Technol. 14, 1041 (1988).

[7] Surrette, R. A., "A novel tritium process monitor that uses an X-ray detector," Nucl. Instrum. Methods A337, 588 (1994).

[8] Shah, K. S., Gothoskar, P., Farrell, R. F. and Gordon, J., "High efficiency detection of tritium using silicon avalanche photodiodes," IEEE Trans. Nucl. Sci. 44, 774 (1997).

[9] Willms, R. S., Dogruel, D., Myers, R. and Farrell, R., "A new solid state tritium surface monitor," Fusion Sci. Technol. 48, 409-412 (2005).

[10] Farrell, R., Shah, K., Vanderpuye, K., Grazioso, R., Myers, R. and Entine, G., "APD arrays and large area APDs via a new planar processing," Nucl. Instrum. Methods A 442, 171-178 (2000).

[11] Farrell, R., Vanderpuye, K., Cirignano, L., Squillante, M. R., and Entine, G., "Radiation Detection Performance of Very High Gain Avalanche Photodiodes," Nucl. Instrum. Methods A353, 176-179 (1994).

[12] Redus, R. and Farrell, R., "Gain and Noise in Very High Gain Avalanche Photodiodes: Theory and Experiment," in Hard X-Ray/Gamma Ray and Neutron Optic Sensors and Applications, R. B. Hoover and F. P. Doty eds., Proc. SPIE 2859, 288-297 (1996).

[13] Christian, J. F., Dokhale, P.A., Lawrence, W.G., Stapels, C.J., Augustine, F.L., Shah, K.S. and Squillante, M.R., "An application-specific integrated circuit for positron emission tomography," IEEE Nuclear Science Symposium Conference Record 5, 2963- 2966 (2005).

*Corresponding Author: Rmyers@rmdinc.com; phone 1 617 668-6821; fax 1 617 926-9980; www.rmdinc.com